ISSN: 2639-7455

Research article

Earth & Environmental Science Research & Reviews

Shoreline changes in Barren Island, India

Shiva Shankar V[1*], Neelam Purti[2], Dharanirajan K[1], Mohan PM[3], Narshimulu, G[4].

[1]*Department of Coastal Disaster Management, Pondicherry University, Brookshabad Campus, Port Blair, Andamans-744112, India.*

[2]*Department of Environment and Forest, Manglutan Range, Port Blair, Andamans-744105, India.*

[3]*Department of Ocean Studies and Marine Biology, Pondicherry University, Port Blair Campus, Andamans-744112, India.*

[4]*Department of Geography, JNRM, Port Blair, Andamans-744103, India.*

[*]Corresponding author
Shiva Shankar, Department of Disaster Management, Pondicherry University, Port Blair Campus, Andaman and NicobarIslands-744112, India.

Submitted: 03 July 2020; **Accepted**: 09 July 2020; **Published**: 17 July 2020

Abstract

Barren Island is the only active volcano in the Indian sub-continent. This study was conducted to understand the changes in the shoreline, which were extracted using the historic after map of [1] and from the time series Landsat images of 1976, 2003 and 2018. End Point Rate (EPR) and Net Shoreline Movement (NSM) were computed using the Digital Shoreline Analysis Software (DSAS) and the ArcMap 10.3 software. The results of mean EPR (9.95m/year) and mean NSM (149.27m) were maximum during volcanic eruption (2003-2018). During dormancy (1885-1976), the mean EPR and NSM values were calculated to be 0.97m/year and 87.89m, respectively. Tropical monsoonal rains, waves and tidal action played a vital role in shaping the shoreline of the island during quiescence apart from volcanic, seismic, and tectonic activity. The estimated values of the extended area of this Island were 827.35 ha and 860.67 ha, respectively, for the years 1885 and 2018. The accretion of lava as a delta in the coastal frontier had dramatically changed the shoreline of the island.

Key words: Shoreline, Volcano, Barren Island, Landsat, DSAS, GIS, North Andaman.

Introduction

Volcanoes are Mother Nature's firework and are the true spectacles of planet earth. It is the core of physical, biological, chemical, atmospheric and cultural evolution of our planet [2-4]. Majority of volcanoes are configured in a curvilinear fashion along the tectonic plate boundaries so called the 'pacific ring of fire' [5]. Approximately half (770) out of the 1550 Holocene active volcanoes are present in Asia (https://www.volcanodiscovery.com/asia.html). Barren Island (BI) is a lone active mafic strato-volcano (figure 1) in the Indian subcontinent (12º 29' N, 93º 85'E). It is located 135km ENE of Port Blair, the capital of Andaman and Nicobar Islands (ANIs) and ~70km east of south Andaman Island [6-8]. The volcanic activity of BI since 1991 happen to change not only the shoreline but also changed the island's coastal geomorphology.

Coastal morphologic changes are a consequence of multifaceted and nonlinear interactions between coastal sediments and dynamic processes such as wind, waves and tides. These interactions occur over an array of time and space scales thus making it a multi-scale phenomenon [9]. A change in coastal geomorphology implies

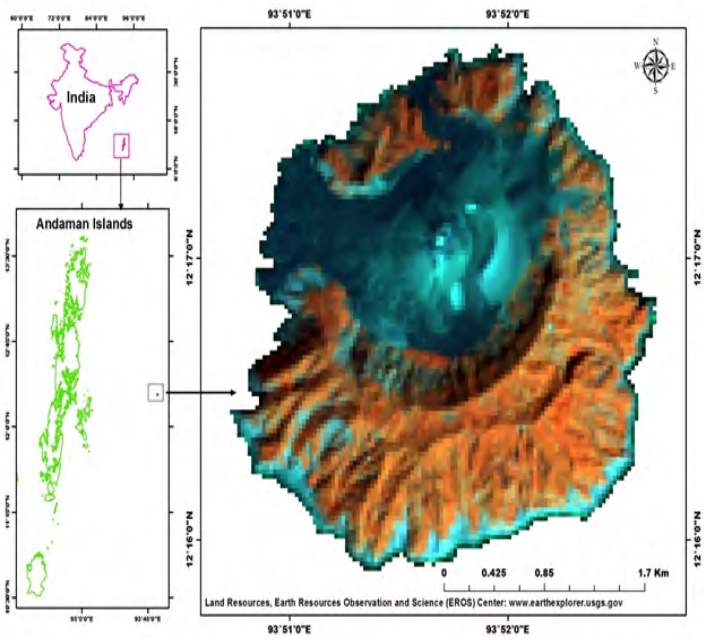

Figure 1: Map showing the study area as on 2018 Landsat-8

change in shoreline. In addition, the change in shoreline may be due to hydrodynamic, geomorphic, tectonic, volcanic and climatic forces [10-12]. Thus, a shoreline is a dynamic coastal geomorphic feature demarcating the boundaries of water and land, having significant relevance to the historical, ecological and economic wealth of a country, also demonstrated by spatio-temporal variations [13]. It has a marked influence of dynamic terrestrial and marine forces that transform the coastal landforms, usually highlighting the changes in long and short time frames [14-19].

Geographic Information System (GIS) and Remote Sensing (RS) are indispensable, cost-effective, relatively accurate and appropriate tools for the quantification of historical changes in the shoreline be [19-25]. Landsat series of satellite data provide reliable results in quantifying geomorphic and shoreline changes [26-30]. A literature survey (Supplementary document) clearly suggests that there are voluminous works pertaining to geology, tectonic setup and geo-chemical studies with few works on the impact of volcanic eruption on regional climatic condition, faunal, floral diversity and plant growth promoting bacterial diversity of the BI. However, there is a paucity of studies on the shoreline change of BI. Therefore, the present study was carried out Using GIS and remote sensing to estimate changes in the shoreline of BI.

Study area - Geology and Climate

BI is roughly circular and rises from a water depth of ~2,300m to a height of ~355m above the mean sea level [31]. The volcanic activity in this island is dynamically changing the area and its shoreline with the island having an average area of 8.60 sqkm as of 2018 and ~3km across. BI is situated on the chain of active volcanoes of Java, Sumatra and extinct volcanoes of Myanmar, which have been acknowledged as the Neogene inner arc volcanic belt of South East Asia [32, 33]. The first documented eruption of the Island, dates back to 1787 and lasted till 1832 [31, 34]. After 159 years of quiescence, the BI showed signs of breathing fire in 1991 [35], since then the volcano has been actively spewing lava (1991, 1994-1995, 2005-2006, 2008-2009, 2017-2018, 2019) and has been reported periodically [7, 36, 37]. The Hawaiian and Strombolian types of eruption were both observed in succession [8, 34]. Recently, the Strombolian type of activity with frequent moderate-to-low scale ash eruptions, lava eruptions were occasionally observed [37]. Aa-aa lava flow from recent eruptions had masked the first recorded historic (1787-1832) flows, drained into the sea accreting a sizable lava delta [7, 8, 31, 36] and thus, altering the shoreline along with the geomorphology of the island.

Late Pleistocene time eruption resulted in the emergence of this volcanic island [34]. The prehistoric cone has an estimated elevation of 1100m, with its base having a diameter of about 12 km while the caldera wall has an outer slope of approximately 32° [38]. The volcano has a nearly circular caldera of ~2 km diameter, with a rupture in the caldera wall on the north western side, which has existed at least since 1787 [7]. Six lava flows separated by scoria beds, minor tuff and cinder deposits are visible on the caldera wall [38]. Rocks, which originated from historic volcanic activity, were composed of basaltic to basaltic andesite [31]. However, recent eruptions have resulted in porphyritic basaltic to andesitic dominated by plagioclase phenocrysts [39].

Since the island is located in the tropical belt, it is frequently battered by meteorological events by both the southwest (May to September) and northeast (October- December) monsoon. A 50-year average of the meteorological data indicates that the island receives 3000mm of rain in 135 rain days in a year. The mean relative humidity was recorded to be 79% with the temperature ranging between 23.8 and 30.2°C.

Materials and Methods

Dataset

Owing to the small areal dimension of the BI shoreline, it is significant in terms of coastal and island ecology. One scene each of the Landsat-2 Multispectral Scanner (MSS), Landsat-7 Enhanced Thematic Mapper Plus (ETM+), and Landsat-8 Operational Land Imager /Thermal Infrared Sensor (OLI/TIRS) images were collected from the United States Geological Surveys (USGS), Earth Explorer (http://www.earthexplorer.usgs.gov) for a period from 1976, 2003 and 2018, respectively. These satellite images were used to study shoreline changes in BI, apart from the historic 1885 map of [1]. Cloud free satellite images were carefully chosen with a valid supporting reason. Landsat-2 (1976) was the first ever satellite data available for the area under consideration. After 159 years of dormancy, the island started erupting since 1991; therefore, 2003 ETM satellite images was chosen. The OLI/TIRS2018 satellite image will give a window of the current status of the island.

Methodology

ArcGIS 10.3 and DSAS 4.3 were used to comprehend the objectives of the present study. It involves three steps namely: (1) Pre-processing, (2) Delineation of historic shorelines and (3) Quantification of shoreline displacement. Pre-processing involves two steps, namely: 1) Removal of gaps or scan-line errors and 2) Co-registration. The scan-line errors of 1976 Landsat imagery were fixed using Landsat toolbox. Individual bands of 1976 Landsat MSS were fixed for scan-line error, thereafter; a composite image was obtained by stacking all the bands together using an image-processing tool. [1] historic map was co-registered with the satellite imagery and re-projected to the real world coordinate system of the Universal Transverse Mercator (UTM zone 46N) with reference datum as WGS1984. Historic shorelines (1885, 1976, 2003 and 2018) were delineated from the pre-processed satellite images. In order to calculate End Point Rate (EPR) and Net Shoreline Movement (NSM) in DSAS, all the shorelines were appended to a single feature class.

DSAS is a plug-in functionality of the ArcGIS software used for quantifying shoreline displacement from the multi-date satellite imageries developed by [40] for the United States Geological Surveys. The plug-in demands three important steps, viz., baseline definition, generation of perpendicular transects parallel to the coast, which in turn compute the rates of shoreline changes by using the least median of squares. The results such as NSM and

EPR were generated from the software. The baseline was manually generated on the coast, in respect to being parallel to the dominant tendency of four different periods of shorelines. In order to understand the major shoreline displacements, transects of 750m length from the baseline were set at 25m spacing alongshore, which means that the shoreline range rates were calculated every 25m along the lava delta. A total number of 63 transects were automatically generated, and statistics were extracted for a 90% confidence interval. As a result of recent intense volcanic activity, heavy monsoonal rains, being remotely situated and strategically important, entry into BI for scientific investigation is restricted historic map served as a reference to begin the investigation, along with remote sensed USGS satellite data products [1, 41-43].

Results of shoreline changes

Parameters such as EPR and NSM were derived from DSAS in order to quantify the shoreline changes of four different periods like 1885, 1976, 2003 and 2018. EPR is the distance between the oldest and the youngest shoreline divided by the year lapsed between two shorelines. NSM is the total distance between the oldest and the youngest shoreline. Shoreline change was observed only across the lava delta of BI. Hence, to assess the shoreline change, a total of 63 transects were generated with a spacing 25m across it. There are 19 transects (36-55) in 1885-1976 and 1976-2003. Whereas, 63 transects (4-67) in 2003-2018. EPR and NSM were calculated for BI using the same boundaries for 1885, 1976, 2003 and 2018 (figure 2, figure 3, figure 4 and figure 5). Accretion of lava delta for 1885-1976, 1976-2003 and 2003-2018 are described (table 1).

SLC between 1885 -1976

This period span of 91 years, wherein BI activities were dormant. The minimum, maximum and mean EPR values were calculated to be 0.01, 1.78 and 0.97m/y, respectively. Also, the minimum, maximum and mean NSM values were estimated to be 0.21, 160.5 and 87.89m, respectively, suggesting that the shoreline very slowly migrated seawards (figure 2a, figure 2b and figure 3). Alteration of the shoreline of BI was trending from NW to W (figure5a and figure 5b). The movement of the shoreline was observed from 36 to 55 transect ID's. The length of shoreline was estimated to be 0.91km and 1.09km for the year 1885 and 1976 respectively. During 91 years of quiescence (1885-1976) 6.89ha of lava delta was accreted to BI. Thus, altering the areal extent of the island from 827.35ha (1885) to 834. 24ha (1976).

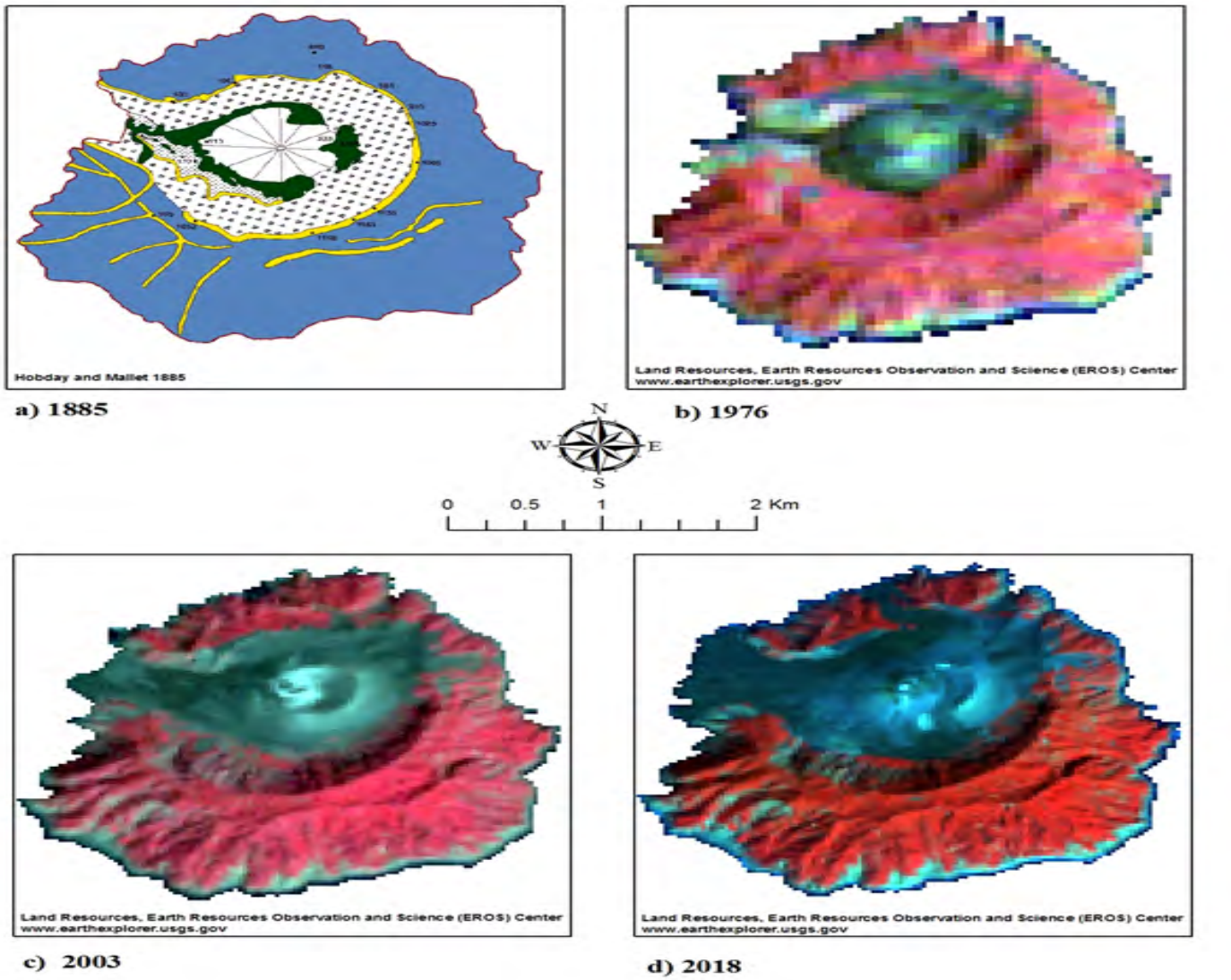

Figure 2: a) Hobday and mallet's 1885 historic map, b) 1976-Landsat –MSS data, c) 2003-Landsat-7 ETM+ and d) 2018- Landsat-8 OLI/TIRS.

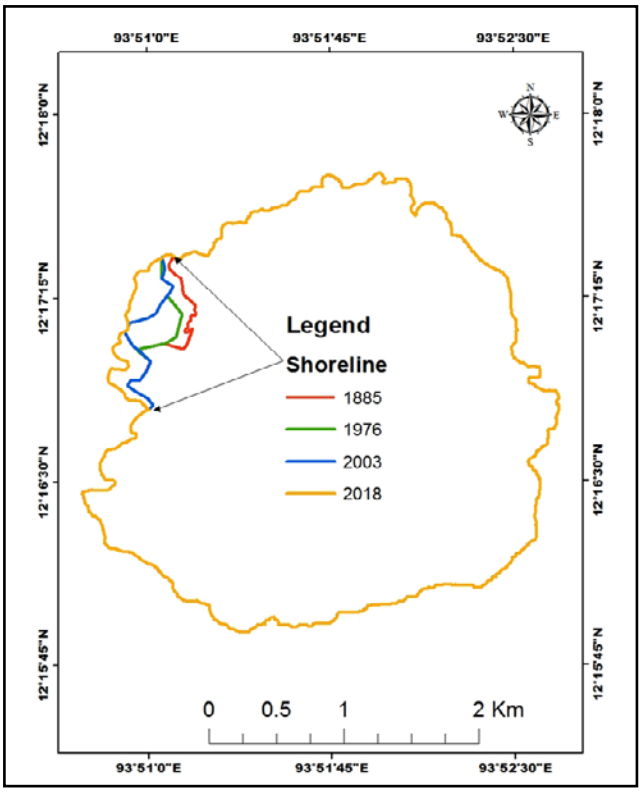

Figure 3: Map showing shorelines of the years 1885, 1976, 2003 and 2018

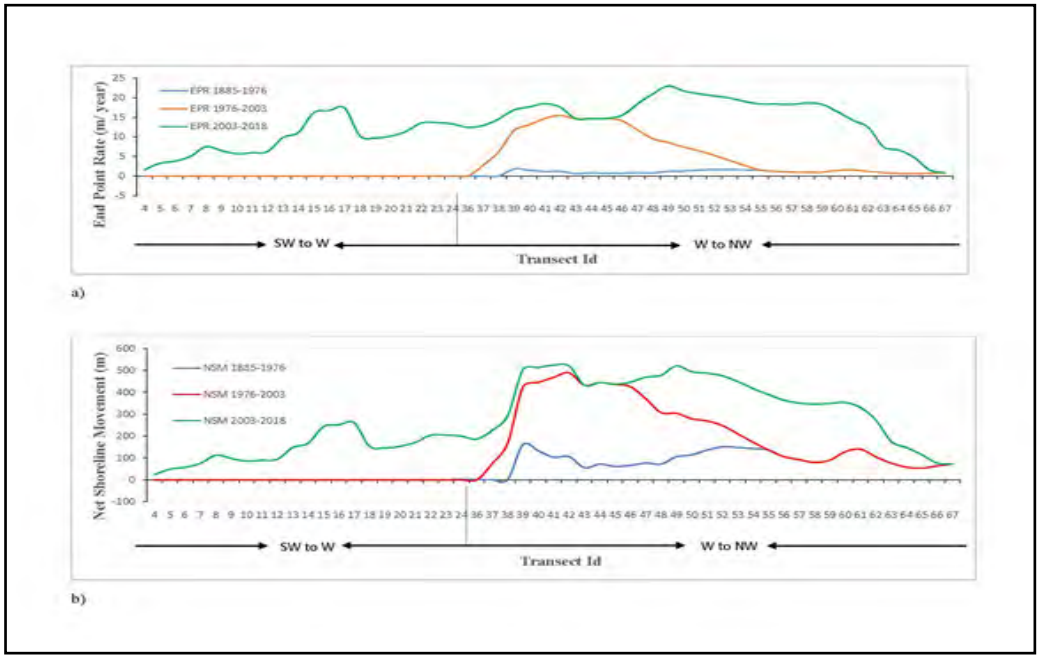

Figure 4: a) End Point Rate b) Net Shoreline Movement with respect to time period of (1885-1976), (1976-2003) & (2003-2018).

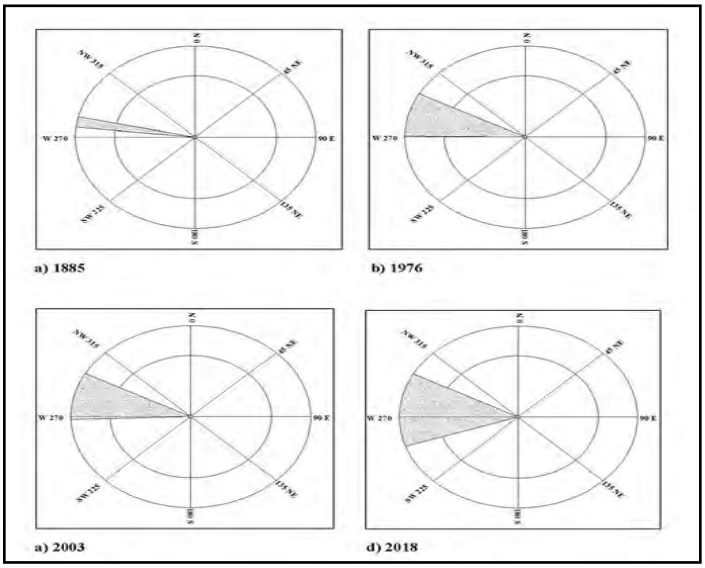

Figure 5: Rose diagram representing the shoreline change direction a) 1885, b) 1976, c) 2003 and d) 2018.

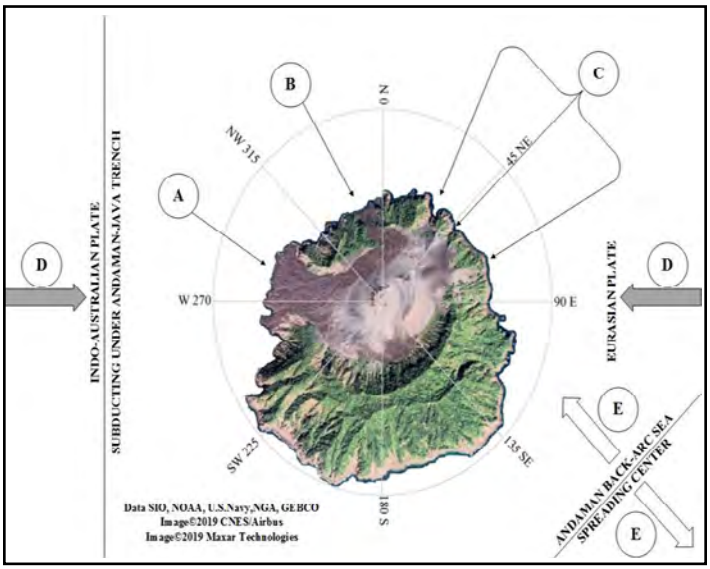

Figure 6: A) Old lava delta since 1885 actively accreting as on date, B) Post tsunami (2005) new lava delta actively accreting, C) Anticipated future site for new lava delta, D) Grey arrow- Convergent plate boundary, E) White arrow Andaman back-arc sea spreading center.

SLC between 1976-2003

BI experienced three phases of shoreline changes during this period viz., 15 years of quiescence (1976-1991), thereafter three years of intense volcanic activity (1991, 1994-1995) and ten years of inter eruption period totally accounting for 27 years. This periodic alteration of the shoreline was observed between 36 to 55 transect ID's unlike what was observed during the period between 1885-1976 events. The minimum, maximum and mean ERP were calculated to be 1.08, 14.27 and 8.83 m/year, respectively. In addition, the minimum, maximum and mean NSM were 29.09, 383.1 and 236.97m, respectively. A significant variation was observed in the movement of shoreline towards the sea (figure 2b, figure 2c and figure 3). The expansion of lava delta was trending (figure 5b and figure 5c) from NW-W (1885-1976) to W-SW (1976-2003). The calculated length and change in area of shoreline was 1.12km (2003) and 9.24ha (1976-2003) respectively. The area of BI thus, was estimated to be 843.48ha (2003).

SLC between 2003 -2018

This duration was purely dominated by episodes of intense volcanic (2005-2006, 2008-2009, 2017and 2018) and inter eruption periods. The minimum, maximum and mean ERP values were calculated to be 0.05, 17.73 and 9.95m/year, respectively. In addition, the minimum, maximum and mean NSM were 0.72, 265.95 and 149.27m, respectively. Dramatic changes in the shoreline were observed in a span of 15 years between transect IDs 4 to 67. However, the shoreline trending not only changed from NW-W to W-SW (figure 5c and figure 5d) but also extended seawards (figure 2c, figure 2d and figure 3). The area of BI was assessed to be 860.67ha during 2018. As the estimated change in area and length of the shoreline to be 17.19ha and 1.73km respectively.

Discussion

The lava delta of BI has been changing rapidly (table 1, figure 2 and figure 3). The assessment in shoreline of BI was made using publically available satellite data products, perceivable changes in shoreline was observed along the lava delta during this study. BI being a strato-volcano, pyroclastic debris are emplaced on the steep gradient [7, 8, 35, 37, 44]. This pyroclastic debris were rapidly dislodged and escorted by heavy tropical rains, thereby contributing to epiclastic accretion at the coastal frontiers [45]. In fact, a discrete chemical reaction is triggered between rainwater and the pyroclastic debris resulting in a concrete like slurry called 'lahar' [8] and can reach a considerable speed, depending upon the chemical composition of the pyroclastic debris and the slope towards the shoreline [46]. The velocity of the lahar flow is defined by the ratio of pyroclastic debris to water [45]. At the coastal frontiers, other factors such as strong waves and tides play a key role in shaping the lava delta [47-50]. Waves and tides are attenuated to lower rates as its increase near shore water depths result in the exodus of a breaker zone near the coast. Consequently, less energy is expended by the waves to cross the turbulent surf zones and more energy is released over the cliff foot [51]. The pounding of high-energy waves at the cliff foot results in undermining and finally, the cliff collapses onto the adjacent sea to accrete landmass to the island edifice [52].

The Andaman–Nicobar region lies in seismic zone V [53] and is part of the interface between the Indo-Australian plate, the Burma micro-plate and the Eurasian plate on the other side that have experienced moderate-to-large magnitude earthquakes during recent and historic setting for the occurrence of mega thrust earthquakes [54]. BI lies on one of the principal lines of weakness on the earth's surface, which in turn experiences high magnitude earthquakes [55]. The Indo-Australian plate moves at 15±3mm/year in the NE direction [53]. The NE-moving Indo-Australian Plate currently subducts beneath the Eurasian Plate around 250 km west of the BI and the length of the Andaman Trench is 1100 km [7, 32, 56]. The subduction rate varies from 5.7, 5.0 and 3.9 cm/yr in Java, Sumatra and near the Andaman Island, respectively [57-60]. The subduction angle is almost parallel to the Andaman Islands [61]. However, the tectonic scenario is complicated by the presence of active back-arc spreading in the Andaman Sea ESE of BI [7]. As a result of being located close to the Andaman sea spreading cen-

ter (Trending NW to SE) on the Burmese micro plate, BI not only experiences compressional force due to both the converging plate boundaries but also from the back-arc spreading center. This results in the formation of several cracks and fissures on the volcanic cone [62].

The compressional force resulted in the vertical collapse of crater and it would have occurred some times in the prehistoric period such as the late Pleistocene [34] and a rupture in the caldera wall on the northwestern side, had existed at least since 1787 [7]. The presence of NNE-SSW trending dyke offers some resistance to the compressional force of convergent plate boundaries and the NW-SE trending Andaman sea spreading center [38]. Thus, the continued compressional force resulted in the formation of a new fissure on the NNW of the cone. Lava flow was observed on both the old NW flank which existed at least since 1787 and the new NNW flank of the Island post tsunami (2005) volcanism [7, 63, 64]. Lava flow on the NW trending old flank is parallel to the compressional force of the convergent plate boundaries but orthogonal to the force exerted by the Andaman Sea spreading center [65]. However, the new NNW trending lava flow is perpendicular to the convergent plate boundaries and parallel to the compressional force offered by the Andaman sea spreading center [66]. Also, three new lava flow channels may be created in the future towards the NE of BI (figure 6). Hence, the peculiar behavior of lava flow of BI clearly articulates the local and regional stress regimes, which have a marked influence on the development of fissures, cracks and collapse of calderas within the volcanic edifice [67]. Active tectonism and seismicity have a marked influence on the accretion of lava delta through landslides at the coastal fronts [68, 69]. The movement of lava through different channels will alter the shoreline of BI at different locations in totality in future.

The recent volcanic activity preceded by earthquakes would been resulted in collapse of the cone and movement of volcanic debris towards the sea, thus altering the shoreline of BI [70, 71]. Volcanism is the prime factor that alters the coastal frontlines very rapidly and dramatically. It is dependent on the nature, type, intensity and density of lava flow over time and space [69]. Effusive volcanism as in the case of BI accretes landmass to the island edifices actively contributing to expanding shorelines by approximately 250m [7, 64, 72-76]. The lava flow was heading towards the sea at a velocity of ~2 m/hour on 11 May 1995 [77]. A comparison of the EPR and NSM values of 1885-1976, 1976-2003 and 2003-2018 clearly articulates the shift in the lava delta of BI was due to natural events like the tectonic, volcanic and seismic activity apart from the mass-wasting, waves, tides and constant tropical monsoonal rains on the lava delta and lava debris [69, 78]. Thus, the quantification of shoreline changes of BI clearly suggested that the land area of BI has increased considerably due to the accretion of lava delta [79].

Table 1: Details of shoreline change rate with respect to time period of (1885-1976), (1976-2003), (2003-2018) & (1885-2018).

Year	Transect ID	Min EPR (m/year)	Max EPR (m/year	Mean EPR (m/year)	Min NSM (m)	Max NSM (m)	Mean NSM (m)	Area of Shoreline change (ha)
1885-1976	36 to 55	0.01	1.78	0.97	0.21	160.5	87.89	6.89
1976-2003	36 to 55	1.08	14.27	8.83	29.09	383.1	236.97	9.24
2003-2018	4 to 67	0.05	17.73	9.95	0.72	265.95	149.27	17.19
1885-2018	4 to 67	0.01	17.73	9.95	0.21	265.95	149.27	33.32

Year	Shoreline change direction as measured from North azimuth	Angle of lava delta from cone	Length of Shoreline across lava delta (Km)	Total Area of the Island (ha)
1885	283.12^0 to 276.52^0	6.6^0	0.91	827.35
1976	298.75^0 to 270.57^0	28.18^0	1.09	834.24
2003	298.75^0 to 268.08^0	30.67^0	1.12	843.48
2018	298.75^0 to 250.96^0	47.79^0	1.73	860.67

Conclusion

The present investigation concludes that the volcanic activity after 1991 had played a lead role in changing the coastal geomorphology through the accretion of sizable lava delta, thus increasing the area of Barren Island. However, seismic events, tectonic activities, tropical monsoonal rains, waves and tides played a significant role in altering the shoreline during 159 years of quiescence. Thus, DSAS can also be effectively used to assess the rate of flow of lava on an active volcano.

References

1. Hobday JR, Mallet FR (1885) The volcanoes of the Barren Island and Narcondam in the Bay of Bengal; their topography by captain J. R. Hobday, S.C., and Geology by F . R. Mallet. Memoirs of the Geological Survey of India v. XXI, Pt 4: 251-286.
2. Kasting JF, Catling, D (2003) Evolution of a habitable planet. Annual Review of Astronomy and Astrophysics. 41: 429-463.
3. Mather TA (2015) Volcanoes and the environment: Lessons for understanding Earth's past and future from studies of present-day volcanic emissions. Journal of Volcanology and Geo-

thermal Research, 304: 160-179.
4. Casadevall JT, Tormey D, Sistine VD (2019) Protecting our global volcanic estate: Review of international conservation efforts. International Journal of Geoheritage and Parks 7: 182-191.
5. Cottrell E (2015) Global Distribution of Active Volcanoes. Volcanic Hazards, Risks, and Disasters.
6. Chandrasekharam D, Orlando V, Capaccioni B, Alam MA (2003) Cold springs of the Barren Island, Andaman Sea, Indian Ocean. Current Science, 85: 136-137.
7. Sheth HC, Ray SJ,Bhutani R, Kumar A, Smitha RS (2009) Volcanology and eruptive styles of Barren Island: an active mafic stratovolcano in the Andaman Sea, NE Indian Ocean. Bulletin of Volcanolgy, 71: 1021-1039.
8. Sheth HC, Ray JS, Kumar A, Bhutani R, Awasthi N (2011) Toothpaste lava from the Barren Island volcano (Andaman Sea). Journal of volcanology and Geothermal Research, 202: 73-82.
9. Karunarathna H, Reeve ED (2013) A hybrid approach to model shoreline change at multiple timescales. Continental Shelf Research, 66: 29-35.
10. Scott DB (2005) Coastal changes, rapid. In M. L. Schwartz (Ed.), Encyclopedia of coastal sciences (pp. 253–255). Dordrecht: Springer.
11. Thom BG, Cowell PJ (2005) Coastal changes, gradual. In M. L. Schwartz (Ed.), Encyclopedia of coastal sciences (pp. 251–253). Dordrecht: Springer.
12. Mahapatra M, Ratheesh R, Rajawat AS (2014). Shoreline Change Analysis along the Coast of South Gujarat, India, Using Digital Shoreline Analysis System. Journal of the Indian Society of Remote Sensing.
13. Natesan, U, Thulasiraman N, Deepthi K, Kathiravan K (2013) Shoreline change analysis of Vedaranyam coast, Tamil Nadu, India. Environmental Monitoring & Assessment 185: 5099-5109.
14. Larson M, Kraus NC (1995) Prediction of cross-shore sediment transport at different spatial and temporal scales. Marine Geology 126: 111-127.
15. Miller JK, Dean RG (2004) A simple new shoreline model. Coastal Engineering, 51: 531-556.
16. Sunarto S (2004) Geomorphic changes in coastal area surround Muria Volcano. Dissertation, Gadjah Mada University, Yogyakarta.
17. Mills JP, Buckley SJ, Mitchell HL, Clarke PJ, Edwards SJ, et al. (2005) A geomatics data integration technique for coastal change monitoring. Earth surface processes and landforms, 30: 651-664.
18. David IT, Mukesh MV, Kumaravel S, Sabeen HM (2016) Long- and short-term variations in shore morphology of Van Island in Gulf of Mannar using remote sensing images and DSAS analysis. Arabian Journal of Geosciences, 9: 756.
19. Ram AB, Chandrasekar N, Kaliraj S, Magesh NS (2016) Shoreline change rate and erosion risk assessment along the Trou Aux Biches–Mont Choisy beach on the northwest coast of Mauritius using GIS-DSAS technique. Environmental Earth Sciences, 75: 444.
20. Martin PH, LeBoeuf EJ, Dobbins JP, Daniel EB, Abkowitz MD, et al. (2005) Interfacing GIS with water resource models: a state-of-the-art review. Journal of the American Water Resources Association (JAWRA).
21. Mujabar S, Chandrasekar N, Immanual JL (2007) Impact of the 26th December 2004 Tsunami along the Coast between Kanyakumari and Ovari, Tamil Nadu, South India. Shore Beach 75: 22-29.
22. Durduran SS (2010) Coastline change assessment on water reservoirs located in the Konya Basin Area, Turkey, using multi-temporal Landsat imagery. Environmental Monitoring & Assessment, 164: 453-461.
23. Mujabar S, Chandrasekar N (2011) Shoreline change analysis along the coast between Kanyakumari and Tuticorin of India using remote sensing and GIS. Arabian Journal of Geosciences.
24. Kaliraj S, Chandrasekar N, Magesh NS (2013) Evaluation of coastal erosion and accretion processes along the southwest coast of Kanyakumari, Tamil Nadu using geospatial techniques. Arabian Journal of Geosciences.
25. Duru U (2017) Shoreline change assessment using multi-temporal satellite images: a case study of Lake Sapanca, NW Turkey. Environmental Monitoring & Assessment, 189: 385.
26. White K, El Asmar HM (1999) Monitoring changing position of coastlines using Thematic Mapper imagery, an example from the Nile Delta. Journal of Geomorphology, 29: 93-105.
27. Srinivasa KT, Mahendra RS, Nayak S, Radhakrishnan K, Sahu KC (2008) Coastal vulnerability assessment for Orissa State, East coast of India. Journal of Coastal Research, 26: 523-534.
28. Meur-Ferec C, Philippe D, Valerie M (2008) Coastal risks in France: an integrated method for evaluating vulnerability. Journal of coastal research, 24: 178-189.
29. Mwakumanya AM, Munyao TM, Ucakuwun EK (2009) Beach width analyses in beach erosion hazard assessment and management at Bamburi beach, Mombasa, Kenya. Journal of Geography and Regional Planning, 2: 299-309.
30. Marghany M, Sabu Z, Hashim M (2010) Mapping coastal geomorphology changes using synthetic aperture radar data. International Journal of the Physical Sciences 5: 1890-1896.
31. Luhr JF, Haldar D (2006) Barren Island volcano (NE Indian Ocean): Island-arc high-alumina basalts produced by troctolite contamination. Journal of Volcanology and Geothermal Research, 149: 177-212.
32. Curray JR (2005) Tectonics and history of the Andaman Sea region. Journal of Asian Earth Sciences, 25: 187-232.
33. Bandopadhyay PC, Gosh B, Limonta M (2014) A reappraisal of the eruptive history and recent (1991-2009) volcanic eruptions of the Barren Island, Andaman Sea. Episodes, 37: 192-205.
34. Shanker R, Haldar D, Absar A, Chakraborty SC (2001) Pictorial monograph of the Barren Island volcano: the lone active volcano in the Indian subcontinent. Geological Survey of In-

dia Special Publication, 67: 87.
35. Ray JS, Pandey K, Awasthi N (2013) A minimum age for the active Barren Island volcano, Andaman Sea. Current Science, 104: 934-938.
36. Sheth HC, Ray JS, Bhutani R, Kumar A, Awasthi N (2010) The latest (2008–09) eruption of Barren Island volcano, and some thoughts on its hazards, logistics and geotourism aspects. Current Science 98: 620-626.
37. Ray D, Shukla DA, Ray JS (2017) Early 2017 activity of the Barren Island volcano: facts versus hype. Current Science, 113: 1657-1659.
38. Alam MA, Chandrasekharam D, V aselli O, Capaccioni B, Manetti P, etal. (2004) Petrology of the prehistoric lavas and dyke of the Barren Island, Andaman Sea, Indian Ocean. In: Magmatism in India through time, (eds: H.C. Sheth, and K. Pande), Proceedings of the Indian Academy of Science (Earth Planet Science) 113: 715-721.
39. Streck MJ, Ramos F, Gillam A, Haldar D, Duncan RA (2011) The intra-oceanic BI and Narcondam arc volcanoes, Andaman Sea: implications for subduction inputs and crustal overprint of a depleted mantle source. In Topics in Igneous Petrology (eds Ray, J., Sen, G. and Gosh, B.), Springer Science : 241-273.
40. Thieler ER, Himmelstoss EA, Zichichi JL, Ergul A (2009) Digital Shoreline Analysis System (DSAS) version 4.0—an ArcGIS extension for calculating shoreline change: U.S. Geological Survey Open-File Report 2008-1278.
41. GVP (Global Volcanism Program) (2005a) Report on Barren Island (India). In: Wunderman, R (ed.), Bulletin of the Global Volcanism Network 30: 5.
42. GVP (Global Volcanism Program) (2008) Report on Barren Island (India). In: Wunderman, R (ed.), Bulletin of the Global Volcanism Network 33: 11.
43. Alam MA (2008) Geological, geochemical an geothermal studies on the Barren Island volcano, Andaman Sea, Indian Ocean: Ph.D. dissertation, Indian Institute of Technology Bombay, Mumbai, India.
44. Alba P Santo (2016) Geochemical data on the 2005 lava flow of Barren Island volcano, Andaman Sea. Current Science 110: 1896-1899.
45. Lirer L, Vinci A, Alberico I, Gifuni T, Bellucci F, et al. (2001) Occurrence of inter-eruption debris flow and hyper concentrated flood-flow deposits on Vesuvio volcano, Italy. Sedimentary Geology, 139: 151-167.
46. Marshak S (2013) Essentials of Geology, 4th edition. W. W. Norton & Company Inc., 500 Fifth Avenue, New York, NY 10110.
47. Awang NA, Jusoh WHW, Hamid MRA (2014) Coastal erosion at Tanjong Piai, Johor, Malaysian Journal of Coastal Research, 71: 122-130.
48. Rajawat AS, Chauhan HB, Ratheesh R, Rode S, Bhanderi RJ, et al. (2015) Assessment of coastal erosion along the Indian coast on 1:25,000 scale using satellite data of 1989–1991 and 2004–2006 time frames. Current Science, 109: 347-353.
49. Ariffin EH, Sedrati M, Akhir MF, Yaacob R, Husain ML, et al. (2016) Open sandy beach morphology and morphodynamic as response to seasonal monsoon in Kuala Terengganu, Malaysian Journal of CoastalResearch,75: 1032–1036,
50. Ashraful IM, Mitra D, Dewan A, Akhter SH (2016) Coastal multi-hazard vulnerability assessment along the Ganges deltaic coast of Bangladesh - a geospatial approach. Ocean and Coastal Management 127: 1-15.
51. Trenhaile AS (2014) Modelling the effect of Pliocene–Quaternary changes in sea level on stable and tectonically active land masses. Earth Surface Processes and Landforms, 39: 1221-1235.
52. Quartau R, Trenhaile S, Ramalho SR, Mitchell CN (2018) The role of subsidence in shelf widening around ocean island volcanoes: Insights from observed morphology and modeling. Earth and Planetary Science Letters, 498: 408-417.
53. Malik NJ, Murty CVR, Rai DC (2006) Landscape Changes in the Andaman and Nicobar Islands (India) after the December 2004 Great Sumatra Earthquake and Indian Ocean Tsunami. Earthquake Spectra 22: S43–S66.
54. Rajendran CP, Earnest A, Rajendran K, Das RD, Kesavan S, et al. (2003) The 13 September 2002 North Andaman (Diglipur) earthquake: An analysis in the context of regional seismicity, Current Science, 84: 919-924.
55. CGWB (Central Ground Water Board) report (2010) Approach paper on ground water quality issues in islands (Andaman & Nicobar and Lakshadweep).
56. Dasgupta S, Mukhopadhyay M (1997) Aseismicity of the Andaman subduction zone and recent volcanism. Journal of the Geological Society of India 49: 513-521.
57. Chlieh M, Avouac JP, Sieh K, Natawidjaja DH, Galetzka J, et al. (2008) Heterogeneous coupling of the Sumatran megathrust constrained by geodetic and paleogeodetic measurements. Journal of Geophysical Research 3: B05305,
58. Cattin R, Chamot Rooke N, Pubellier M, Rabaute A, Delescluse M, et al. (2009) Stress change and effective friction coefficient along the Sumatra Andaman-Sagaing fault system after the 26 December 2004 (Mw= 9.2) and the 28 March 2005 (Mw= 8.7) earthquakes. Geochemistry, Geophysics, Geosystems.
59. Gahalaut VK, Nagarajan B, Catherine JK, Kumar S (2006) Constraints on 2004 Sumatra–Andaman earthquake rupture from GPS measurements in Andaman–Nicobar Islands. Earth and Planetary Science Letters 242: 365-374.
60. McCaffrey R (2009) The tectonic framework of the Sumatran subduction zone, Annual Review of Earth and Planetary Sciences 37: 345-366.
61. Prawirodirdjo L, Bock Y (2004) Instantaneous global plate motion model from 12 years of continuous GPS observations. Journal of Geophysical Research: Solid Earth, 109(B8).
62. Banerjee B, Subba Rao PBV, Gautam G, Joseph EJ, Singh BP, et al. (1998) Results from a magnetic survey and geomagnetic depth sounding in the post-eruption phase of the Barren Island volcano. Earth Planets Space 50: 327-338.
63. GVP (Global Volcanism Program) (2005b) Report on Barren Island (India). In: Wunderman, R (ed.), Bulletin of the Global Volcanism Network, 30: 9.
64. GSI (Geological Survey of India) (2009) The Barren Island Volcano, Explosive Strombolian type eruption observed

during January 2009, Jan 2009 URL:
65. Nakamura K (1977) Volcanoes as possible indicators of tectonic stress orientation - principle and proposal. Journal of Volcanology and Geothermal Research 2: 1-16.
66. Moriya I (1980) "Bandaian Eruption" and landforms associated with it. Collection of articles in memory of retirement of Prof. K. Nishimura from Tohoku Univ : 214-219 (JwE) [66].
67. Siebert L (1984) Large volcanic debris avalanches: characteristics of source areas, deposits, and associated eruptions. Journal of Volcanology and Geothermal Research, 22: 163-197.
68. GVP (Global Volcanism Program) (1992) Report on Barren Island (India). In: McClelland, L (ed.), Bulletin of the Global Volcanism Network, 17: 1.
69. Ramalho RS, Quartau R, Trenhaile AS, Mitchell NC, Woodroffe CD, et al. (2013) Coastal evolution on volcanic oceanic islands: a complex interplay between volcanism, erosion, sedimentation, sea-level change and biogenic production. Earth-Science Reviews, 127: 140-170.
70. GVP (Global Volcanism Program) (1991b) Report on Barren Island (India). In: McClelland, L (ed.), Bulletin of the Global Volcanism Network, 16: 10.
71. GVP (Global Volcanism Program) (2006) Report on Barren Island (India). In: Wunderman, R (ed.), Bulletin of the Global Volcanism Network, 31: 1.
72. Haldar D, Laskar T, Bandyapadhyay PC, Sarkar NK, Biswas JK, et al. (1992a) Volcanic eruption of the Barren Island volcano, Andaman Sea: Journal of the Geological Society of India 39: 411-419.
73. Awasthi N, Ray JS, Laskar AH, Kumar A, Sudhakar M, et al. (2010) Major ash eruptions of Barren Island volcano (Andaman Sea) during the past 72 kyr: clues from a sediment core record. Bulletin of Volcanology, 72: 1131-1136.
74. Siebert L, Simkin T, Kimberly P (2010) Volcanoes of the World: Third Edition, University of California Press, Berkeley 551.
75. GSI (Geological Survey of India) (2011) Barren Volcano in January 2011: An explosive pulsative eruption (Strombolian) still continues,Eastern Region Geological Survey of India URL:
76. GVP (Global Volcanism Program) (2011) Report on Barren Island (India). In: Wunderman, R (ed.), Bulletin of the Global Volcanism Network, 36: 6.
77. GVP (Global Volcanism Program) (1995) Report on Barren Island (India). In: Wunderman, R (ed.), Bulletin of the Global Volcanism Network, 20: 6.
78. Quartau R, Tempera F, Mitchell NC, Pinheiro LM, Duarte H, et al. (2012) Morphology of the Faial Island shelf (Azores): the interplay between volcanic, erosional, depositional, tectonic and mass-wasting processes. Geochemistry, Geophysics, Geosystems, 13: 1-30.
79. Pal T, Ragav S, Bhattacharyya A, Bandopadhyay PC, Mitra S, et al. (2010) The 2005-2006 eruption of the Barren volcano: evolution of basaltic magmatism in island arc setting in Andaman-Java subduction. Journal of Asian Earth Sciences, 43: 112-123.